Journal of Building Engineering 52 (2022) 104441

Contents lists available at ScienceDirect

Journal of Building Engineering

journal homepage: www.elsevier.com/locate/jobe

Experimental evaluation on punching shear resistance of steel fibre reinforced self-compacting concrete flat slabs

Nor Fazlin Zamri, Roslli Noor Mohamed *, Dinie Awalluddin, Ramli Abdullah

School of Civil Engineering, Faculty of Engineering, Universiti Teknologi Malaysia, 81310, Johor Bahru, Johor, Malaysia

ARTICLE INFO

Keywords:
Steel fibre
Self-compacting concrete
Flat slab
Punching shear

ABSTRACT

Steel fibre reinforced self-compacting concrete (SFRSCC) consolidates under its own weight and has been shown to have the ability to provide an efficient reinforcement mechanism. The concrete with an adequate amount of steel fibre might increase the load and deformation capacities of the structural elements, particularly the tension dominant members. In this study, eight square slab specimens of the same size and reinforced with an identical and sufficient amount of flexural reinforcement were tested. The variables considered included types of concrete, slab thickness, types of shear reinforcement, and the limiting area of SFRSCC around the column. The results show that SFRSCC flat slabs performed well in terms of punching shear strength, ductility, and crack control. The results also reveal that slabs with SFRSCC within a square area around the column can be as efficient in resisting the punching shear as the ones with the SFRSCC cast over the entire slab.

1. Introduction

Flat slab system offers numerous construction and architectural advantages, which make them a popular choice in reinforced concrete (RC) construction. The construction of the flat slab generally eliminates the use of beams where the slab is supported directly by columns [1]. It also offers simpler formwork and greater clear storey height as compared to beam-column frame construction, leading to substantial savings in construction costs. Despite its simple appearance, this flat slab is susceptible to punching shear failures, which could lead to substantial floor damage and even the worst scenario of structural collapse, such as the collapse of the Skyline Plaza [2], Sampoong department store [3], and the 16-storey apartment building at 2000 Commonwealth Avenue [4].

Generally, the shear capacity of this connection can be enhanced by increasing the slab thickness or using drop panels or column capitals, which is not an economical or practical option, as well as having architectural disadvantages. This is because increasing the slab thickness will also increase the cost and weight of the building. Furthermore, the presence of the drop panel or column head causes changes in slab cross-section and formwork that result in non-uniformity in the floor bottom surface and decreasing clear storey height. Thus, modifying the geometrical properties of the slab is not the only method to increase the punching capacity. Since the 1950s, punching shear has been the subject of an intense experimental effort. Although several methods have been proposed to increase the punching shear capacity of flat slabs, their application is still restricted. For example, traditional shear strengthening using stirrups is only applicable to slabs with a depth greater than 150 mm [5], whereas reinforcement using steel section shear head systems [6,7], stud type reinforcement [8], shear band system [9] and lattice shear reinforcement [10] prolongs the duration and increases the cost of construction.

* Corresponding author.
E-mail address: roslli@utm.my (R.N. Mohamed).

https://doi.org/10.1016/j.jobe.2022.104441
Received 20 December 2021; Received in revised form 26 March 2022; Accepted 26 March 2022
Available online 1 April 2022

In these circumstances, steel fibre reinforced concrete (SFRC) is seen as an alternative in enhancing the punching shear capacity, performance, and cracking control of the flat slab. The steel fibre with an adequate amount has proven its ability to provide an efficient reinforcement mechanism through its bridging action and consequently enhance the integrity of the flat slab [11,12]. Apart from the fibre volume fraction and types of fibre, the efficiency of steel fibre also depends on other factors, such as the casting procedure, and the fresh and hardened state of the concrete. Due to its high specific weight, steel fibre has a higher tendency than other constituents to segregate towards the bottom surface, resulting in a lower fibre content near the top surface of the element [13]. This can be avoided by using high-flowing concrete matrices such as self-compacting concrete (SCC) as the medium to transport the fibre.

Despite the obvious advantages of SCC, relatively few works have been published on the use of steel fibre reinforced self-compacting concrete (SFRSCC) to improve the punching shear resistance of reinforced concrete flat slabs [12,14]. Even though the use of shear reinforcement is four times as labour-intensive as fibrous concrete in the fabrication and casting of the slab [15], it remains a top choice to resist the punching shear stress issue. This is because the use of a fibrous concrete mix is costly as compared to plain concrete. Therefore, further research on this topic is clearly desirable. Apart from the investigation into the effectiveness of steel fibre as a secondary reinforcement in comparison to conventional shear reinforcement, this study also investigated the limiting area of SFRSCC around the column that needs to be provided to produce superior structural performance.

2. Experimental works

2.1. Material and concrete properties

The RC flat slabs were cast with three types of concrete: normal vibrated concrete (NC), self-compacting concrete (SCC) and steel fibre reinforced self-compacting concrete (SFRSCC). The SFRSCC specimens were cast with the same fibre dosage of 59 kg/m^3, which is equivalent to 0.75% of the total volume. The dosage of steel fibre was determined in the preliminary study to be the optimum fibre content due to the consistent performance in both fresh and hardened concrete properties [16,17]. NC was designed following the Department of Environmental (DoE) mix design method for normal concrete [18]. The SCC and SFRSCC were designed based on modifications from previous research [19] and recommendations by the European Guidelines [20]. These concrete compositions are tabulated in Table 1 and were designed to achieve a characteristic compressive strength of 30 N/mm^2 at 28 days. The fresh properties of all of the concrete mixes are tabulated in Table 2. It is worth noting that the fresh properties for all concrete mixes meet the performance standards set out in European Guideline [20].

Ordinary Portland Cement (OPC) with a specific gravity of 3.15 was used as a cementitious material for all the concrete mixes. Local river sand that passed through a 4.75 mm sieve was used as fine aggregate, while the maximum nominal size for crushed granite used for coarse aggregate was 10 mm. As the SCC needs powder content in the range of 400 kg/m^3 to 600 kg/m^3, such a high amount of OPC used in the concrete mix will increase the heat from hydration in the concrete, which would raise the risk of the concrete cracking. Therefore, class F fly ash with a specific gravity of 2.1 was used to replace about 30% of the OPC as suggested by previous researchers [21,22]. The use of fly ash was able to reduce the heat of hydration and was environmentally friendly.

In this study, a hooked-end type of steel fibre with a diameter of 0.58 mm, a length of 35 mm and a tensile strength of 1250 N/mm^2 as shown in Fig. 1 was used in this study. Hooked-end shaped fibre has an ideal compromise between workability and performance requirements as the material has an optimum capacity for preventing cracks while providing better ductility and toughness than other types of fibre. It also exhibits good bond behaviour by creating mechanical interlocks between fibres [23,24]. Two percent of the polycarboxylate ether-based superplasticizer, Sika ViscoCrete-2044 was used to acquire the rheological properties of SCC without any segregation and bleeding. It was categorized as a Type F Admixture per ASTM C494/C494 M [25].

2.2. Specimens details

A total of eight half-scaled model reinforced concrete flat slabs with a dimension of 1650 mm × 1650 mm and a thickness of 125 mm (except for specimen S6 with 100 mm) were cast. This represents the area of the slab surrounding a column and bordered by the line of contra-flexure, which occurred at a distance of 0.22L from the column axis (according to a linear-elastic estimate), where L represents the axis to axis distance between columns. Thus, the experimental model was the half-scaled size of the actual slab supported on columns spaced at approximately 7 m with a span/thickness ratio of 28. This dimension is decided after taking into account the testing capability and economics. In the opinion of the writers, if the punching shear resistance of these slabs can be enhanced, then the results are applicable to all slabs deeper than the chosen depth. The main reinforcement, the size of the column and the length and width of the flat slabs were identical for all specimens. The variables in the study were types of concrete, slab thickness, the plan area of the slab around the loaded column that contained the steel fibre and types of shear reinforcement. The details of the slab specimens are tabulated in Table 3. The slabs, S1 and S2, were the control specimens without shear reinforcement.

Table 1
The concrete composition of NC, SCC and SFRSCC.

Mix	NC	SCC	SFRSCC
Cement (kg/m^3)	426.7	342.4	342.4
Fly ash (kg/m^3)	N/A	146.7	146.7
Fine aggregate (kg/m^3)	986.1	1090	1090
Coarse aggregate (kg/m^3)	743.9	675	675
Water (kg/m^3)	213.3	250	250
Steel fibre (kg/m^3)	0	0	59

Table 2
The fresh and hardened concrete properties of NC, SCC and SFRSCC.

Parameter	NC	SCC	SFRSCC	Requirement limit by [20]
Slump (mm)	55	N/A	N/A	N/A
Slump flow (mm)	N/A	715	685	550–850
V-Funnel (s)	N/A	4.0	8.5	≤25
L- box	N/A	0.93	0.86	≥0.80

Fig. 1. Hooked end steel fibre.

All the flat slab specimens were reinforced with high tensile strength reinforcing bar of diameter 12 mm, spaced at 100 mm in both directions according to design requirements and flexural reinforcement ratio, $\rho = 1.3\%$ (flexural reinforcement ratio for S6, $\rho = 1.5\%$) as shown in Fig. 2. The stirrup and welded inclined bar (WIB) in specimens S7 and S8 were made of a diameter of 6 mm and 8 mm, respectively. A tensile strength test on the reinforcements performed according to [26] shows the average values of 348.0 N/mm^2 for 6 mm diameter bars, 577.2 N/mm^2 for 8 mm diameter bars, and 529.7 N/mm^2 for 12 mm diameter bars, respectively. The symbols "R" and "H" used in Figs. 2, 4 and 5 indicate mild steel with a strength of more than 250 N/mm^2 and high-yield steel with a strength of more than 500 N/mm^2, respectively. The compression cube tests were carried out prior to the punching shear tests and the average data was also tabulated in Table 3.

S4 and S5 were cast to study the limit area of SFRSCC that needs to be provided to produce a similar effect as those with steel fibre over the whole slab panel. This concept was similar to the concept of using high strength concrete in the column head area only. The fibrous concrete was extended to 2d (S4) and 3d (S5) from the column face as shown in Fig. 3. Even though the critical section of the flat slab is stipulated in the standard to be 2d from the column face [27], the boundary area was expanded to 3d because the punching shear crack occurred approximately 3d from the column face in the preliminary test. Since the interface between the fibrous concrete and normal concrete was not located within the critical area, which is 0.5d from the column face, the interface was formed by simultaneously placing fibrous and normal concrete. This interface was formed by placing the temporary border using the plywood, and it was removed immediately after the placing of concrete was completed to avoid the separation between fibrous and normal concrete.

Apart from the fibre reinforcement, the alternative shear reinforcements used in this study were closed stirrup and welded inclined bar (WIB). The dimensions and the arrangement layout of the stirrup are shown in Fig. 4. The WIB was a modified system of the bent-up bar, where the inclined bars were welded in the top and bottom horizontal holders at the required spacing, inclined at 60° with respect to the horizontal axis, as shown in Fig. 5. The more effective inclination of the shear reinforcement would be normal to the diagonal cracks. Therefore, as the inclination of the diagonal crack was normally assumed at 30° [28–30], the normal to the diagonal crack was 60°.

2.3. Experimental setup and testing

The general view of the test setup is shown in Fig. 6. The slab specimen was simply supported along its four sides. The slab specimen was placed on I-steel beam sections with a width of 125 mm and a height of 125 mm along four edges to simulate a simply supported boundary condition. Under this test configuration, the corners of the slab were free to lift. These supporting members were fixed on large steel beam sections on two sides, which were laid on the strong floor of the laboratory. The distance from the centre of the support to the edge of the slab was 62.5 mm on all four sides, resulting in the effective span of the slab being equal to 1525 mm in both

Table 3
Details of reinforced concrete flat slab specimens.

Slab	Types of Concrete	Cube compressive strength, f_{cu} (N/mm^2)	Types of Shear Reinforcement (area of shear reinforcement)	Slab Thickness (mm)	Area of steel fibre provided from column face (mm)
S1	NC	36.4	–	125	–
S2	SCC	40.2	–	125	–
S3	SFRSCC	48.6	–	125	full slab
S4	SFRSCC	45.1	–	125	2d
	SCC	43.3			
S5	SFRSCC	42.0	–	125	3d
	SCC	40.5			
S6	SFRSCC	42.5	–	100	full slab
S7	SCC	44.1	Stirrup (2037.6 mm$^{2)}$	125	–
S8	SCC	45.1	WIB (2414.4 mm^2)	125	–

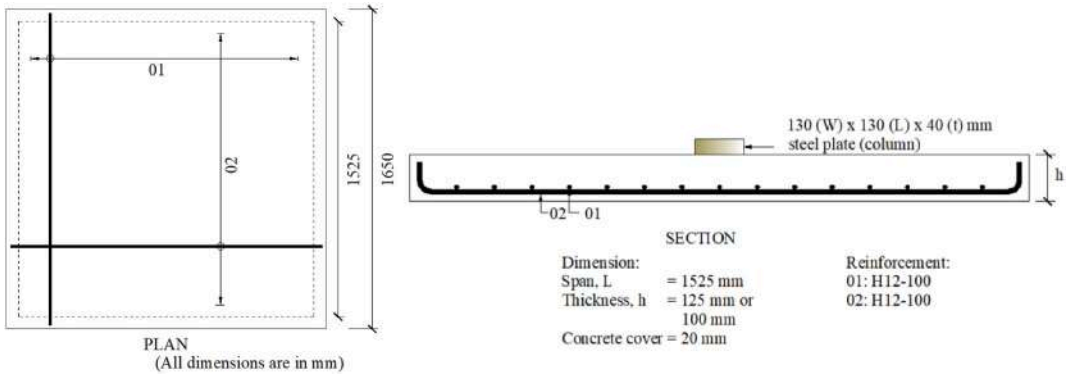

Fig. 2. The reinforcement layout for RC flat slabs.

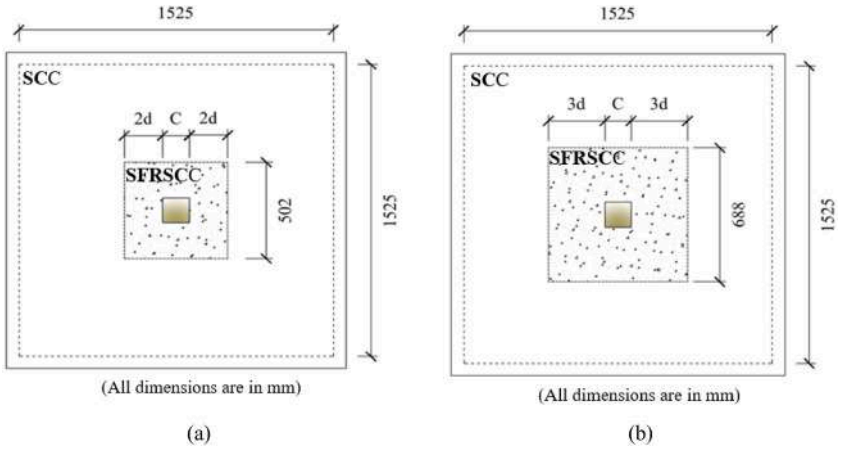

Fig. 3. Plan layout for slabs (a) S4 and (b) S5.

directions. A 130 x 130 × 40 mm steel plate was placed at the middle of the slab to represent the column. The hydraulic jack and the load cell, with capacities of 1000 kN and 500 kN, respectively, were placed on this loading plate in a vertical direction up to the bearing plate of the cross member of the test frame.

Six linear variable displacement transducers (LVDT) were installed near the column face, at quarter and half spans of the slab, and in both the slab's principal directions to ensure the slab surface was evenly loaded as shown in Fig. 7. Strains in steel reinforcements and concrete were measured using TML electric strain gauges with a length of 6 mm and 60 mm, respectively. The positions of steel strain gauges were bonded at the main reinforcement (near the column face and the half span of the slab) as shown in Fig. 8 and shear reinforcement (if needed). The strain gauge was installed in the third row of shear reinforcement at the mid height of the reinforcement bar, as shown in Fig. 9. Meanwhile, the concrete strain gauges were located at the bottom of the slab (tension) near the column face and the half span of the slab as shown in Fig. 10. The load was applied by jacking the slab against the cross beam of the test frame using the hydraulic jack until failure. Halts at 10 kN increments were made to permit recording of the deflection and steel strain and observing the cracks. However, the development of the cracks was unable to be observed closely due to safety reasons. The load was stopped when a sudden failure occurred. At that point, the applied load could not be increased as the hydraulic jack showed decreasing readings.

2.3.1. Fibre distribution and orientation

It is important to check the distribution of fibre around the failure crack to confirm the actual fibre volume fraction in the specimen and the fibre efficiency during post-cracking, which represents the ultimate bridging action. For this purpose, a 50 mm core bit was used to drill the specimen near to the failure crack. A cover metre was used to detect the location of reinforcement, so that the reinforcement area was avoided during the drilling process. Due to the specimen size, it was impossible to analyse the fibre orientation directly on the reinforced concrete flat slab specimen. The number of fibres was counted on the visualised rectangular area on the core specimen and the average of three readings was used in calculating the fibre orientation. Then, the core specimens were crushed to extract the steel fibres. The weight of each core sample was obtained using the hydrostatic weighing method before being crushed. Then, the steel fibres from the crushed concrete cores were extracted by a magnet and weighed. The fibre orientation, η_θ and the fibre volume, V_f fraction were calculated using Equations 1 and 2, respectively.

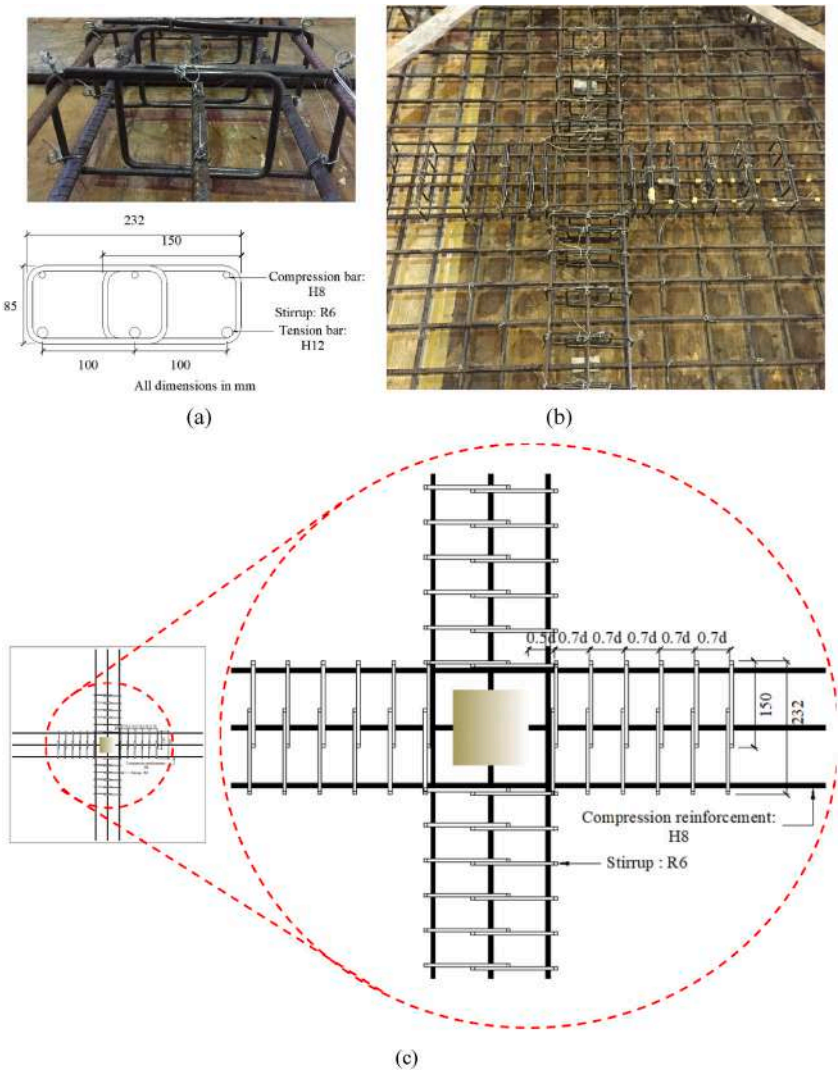

Fig. 4. (a) Stirrup reinforcement details and (b) the elevation view of the WIB reinforcement as it was installed in the slab and (c) stirrup reinforcement arrangement plan layout in slab S7.

$$\eta_\theta = N_1 \frac{A_f}{V_f} \tag{1}$$

$$V_f = \frac{W_{sf}}{V_{core} x \rho_{sf}} \tag{2}$$

where N_1 is number of fibre per cross-sectional area, A_f is cross-sectional area of calculated steel fibre, W_{sf} is weight of steel fibre (kg), V_{core} is hydrostatic volume of core (m^3) and ρ_{sf} is density of fibre (kg/m^3)

3. Results and discussion

3.1. Comparison of ultimate load and average of mid-span deflection

A comparison was carried out on the average deflection at the mid-span of the slab to study the effectiveness of the steel fibre and shear reinforcement in enhancing the punching shear capacity of the reinforced concrete flat slabs. The average deflection was calculated by taking the average of the readings in both principal directions. The deflection was proportional to the load, and the results revealed that the mid-span deflection was greater than the deflection measured away from the slab's centre. As expected, the largest deflection occurred near the mid-span of the slab, due to the nature and symmetry of the loading system. Therefore, in this article, only the comparison of mid-span load-deflection curves for all specimens are presented in Fig. 11. The summary of the results is tabulated in Table 4. It shows clearly that the inclusion of conventional shear reinforcement (stirrup), welded inclined bar and fibre

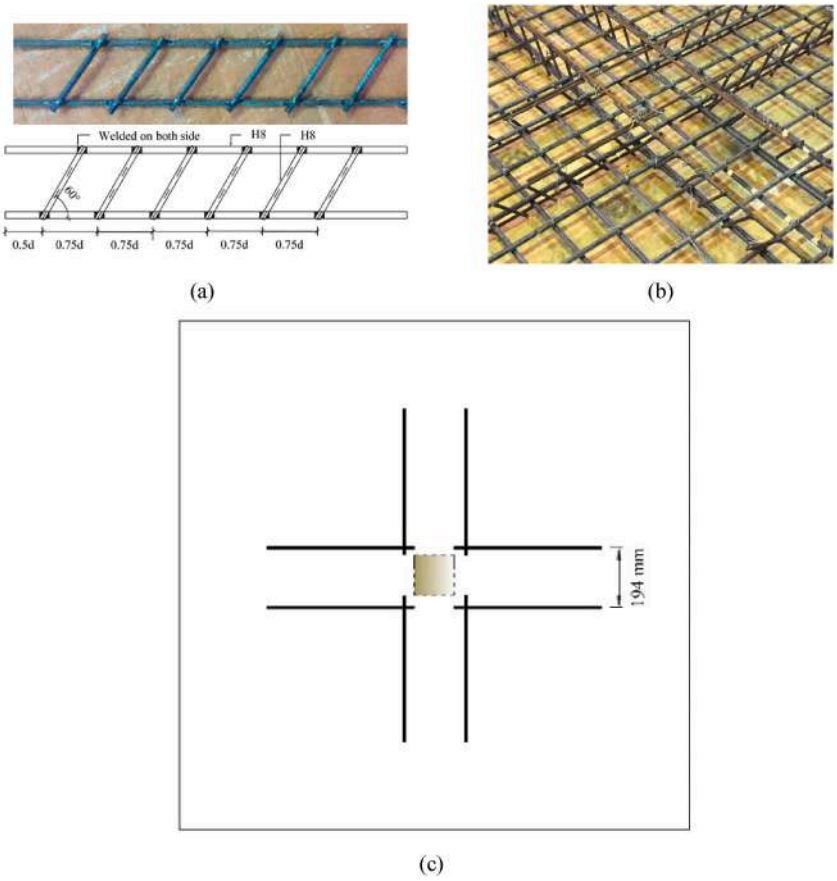

Fig. 5. (a)WIB reinforcement details, (b) the elevation view of the WIB reinforcement as it was installed in the slab. (c) WIB reinforcement arrangement plan layout in slab S8.

reinforcement increase the ultimate load of the slab.

Specimens S1 and S2 were reinforced concrete flat slabs without any forms of shear reinforcement and were used as control specimens. These slabs, which were constructed using normal concrete (NC) and self-compacting (SCC) and tested to evaluate the self-compactibility effect on the structural capacity, showed very little difference. Slab S2 failed at 305.6 kN, which is 5.3% higher than the failure load of slab S1. Nevertheless, both specimens showed similar failure behaviour. Both specimens failed suddenly by punching, indicating very low ductility and residual strength.

Generally, all the slabs show the same behaviour during pre-cracking stage, where the load-deflection curves were approximately linear with a constant gradient. At the ultimate load, the deflection of the fibrous specimens (S3, S4 and S5) was higher than that of the control specimens, S1 and S2. To make a clear comparison of the load-deflection behaviour of slabs, the deflection of each specimen at a randomly selected load of 100 kN is measured and presented in Table 4. At the same loading level, the deflection of slabs reinforced with fibre reinforcement (except slab S6) are lower than the deflection of the control specimens. It shows that the fibre reinforcement has enhanced the stiffness of the slab. The stiffness increment in SFRSCC slabs is related to the improved tensile behaviour of the cracked sections, where the presence of steel fibre in the concrete matrix leads to the improvement of the tensile post-cracking behaviour.

The control specimens, S1 and S2, which had no fibre, failed at 290.1 kN and 305.6 kN, respectively. Slab S3, which was designed with the same reinforcement layout plus $V_f = 0.75\%$, achieved the highest ultimate load of 412.1 kN, which is about 42.1% and 34.8% higher than control specimens S1 and S2, respectively. The fibre has a favourable effect on both cracking capacity and ultimate capacity, which persist from the fibre bridging action in the concrete matrix. Other than the known beneficial effect of fibre bridging action in resisting the propagation of cracks, the tensile zone of SFRSCC slabs also takes part in carrying loads in the early stage of initiation and propagation of cracks. Due to the convincing increase in ultimate load in specimen S3, specimen S6 was cast to evaluate the performance of the thin slab. Specimen S6 failed at 222.3 kN, which is 27.3% lower than the capacity of the control specimen, S2. This is to be anticipated, as the load capacity of the slab is directly proportional to its thickness.

One aspect that should be pointed out is that the steel fibre in specimens S4 and S5 is only provided in the concrete composition in the central square region. Despite these specimens, S4 and S5 failed at about 354.9 kN and 365.6 kN, respectively, which are about 16.1% and 19.6% higher than the control specimen, S2. None of these specimens failed at the interface between the fibre reinforced

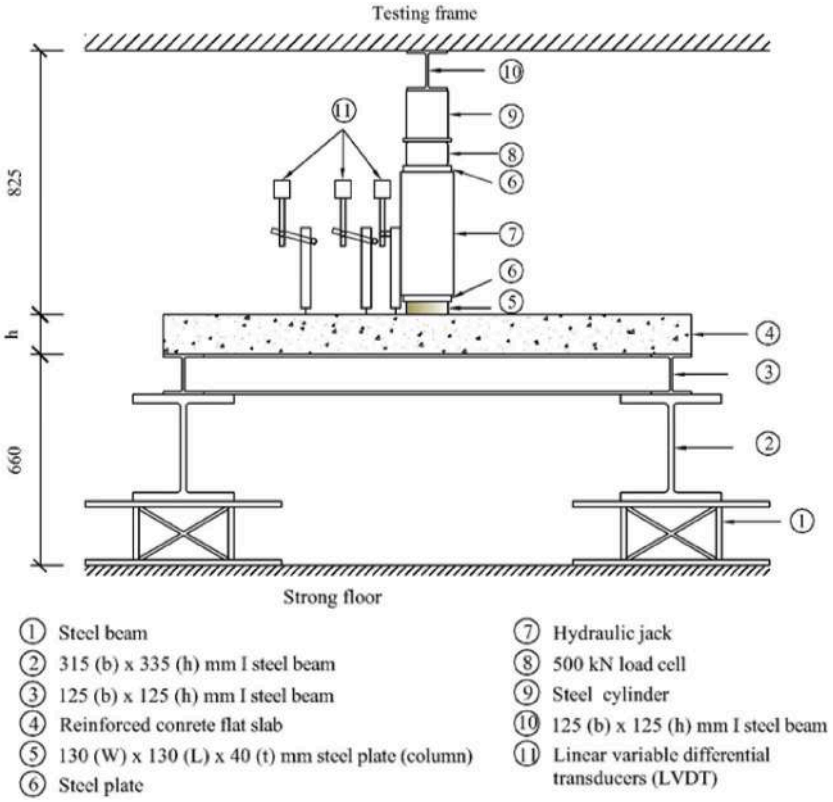

Fig. 6. The schematic diagram of punching shear setup.

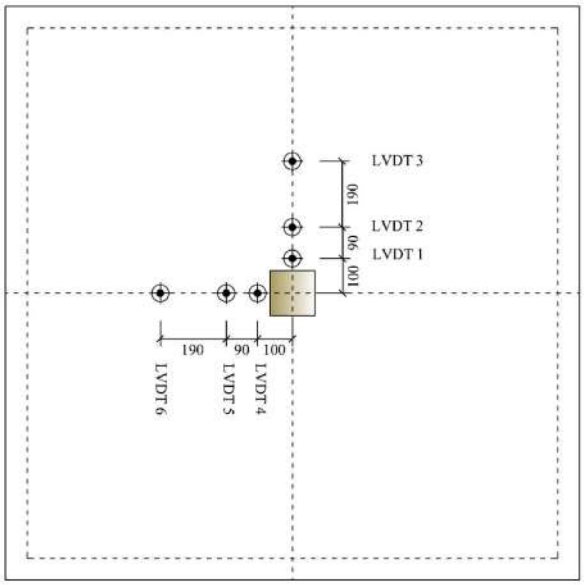

Fig. 7. The location of LVDTs.

concrete region and the surrounding normal concrete (SCC) region of the slab. The circumferential cracks in S4 occurred within the SCC region, while the circumferential cracks in S5 occurred within the SFRSCC region. These results indicate that the use of SFRSCC can be restricted to the region where it is most needed, that is within 2d to 3d from the column face.

Specimens S7 and S8, which were tested to study the effectiveness of different types of shear reinforcement in enhancing the

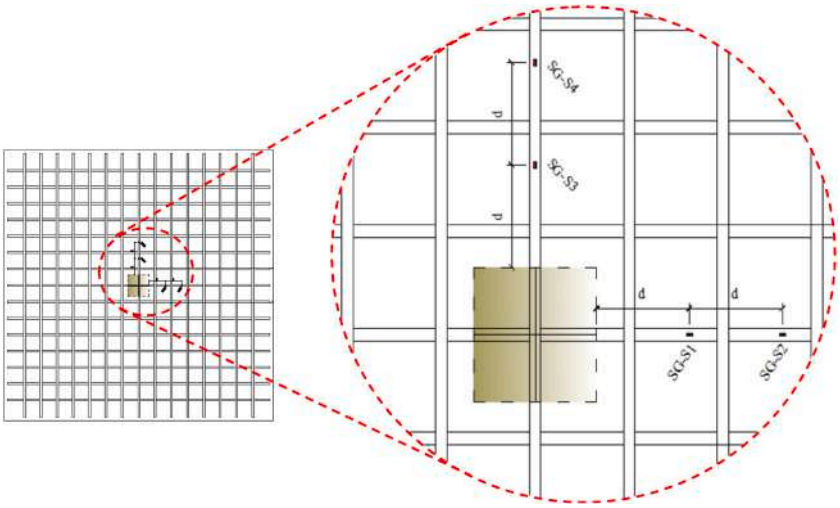

Fig. 8. The location of steel strain gauge.

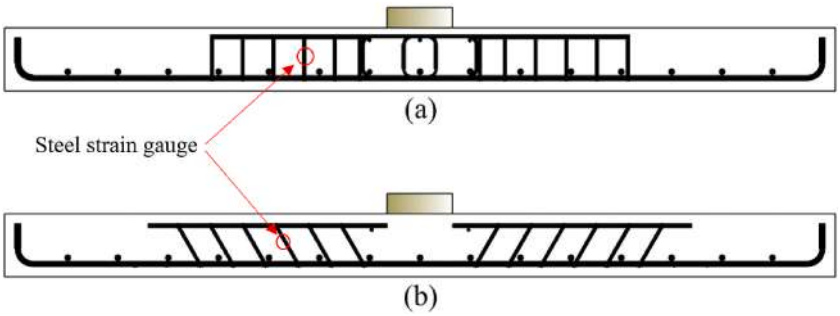

Fig. 9. The location of steel strain gauge in (a) stirrup (S7) and (b) WIB (S8).

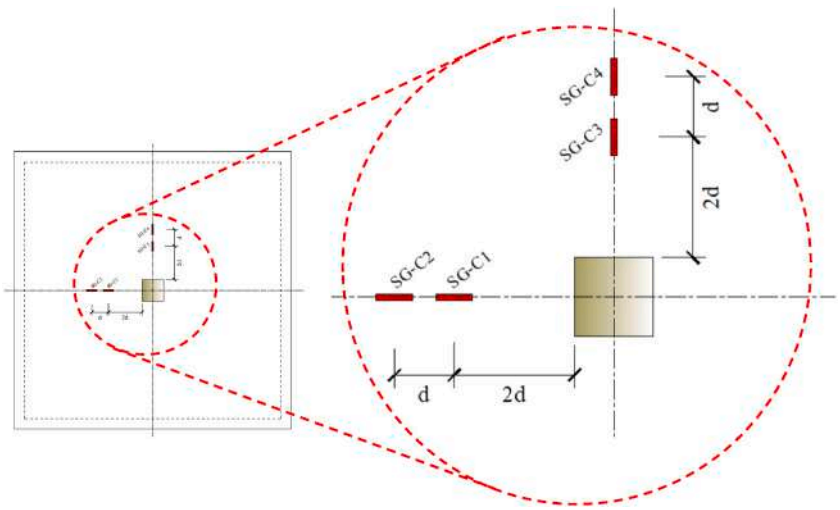

Fig. 10. The location of concrete strain gauge.

punching shear capacity, showed very little difference. Specimens S7 and S8 failed at 336.5 kN and 345.2 kN, which are respectively 10.1% and 13.0% higher than the failure load of the control specimen, S2. On the other hand, the ultimate strength of both slabs was lower than the ultimate strength of fibrous slabs with identical reinforcement layout (S3, S4 and S5). The simplified "beam layout", in

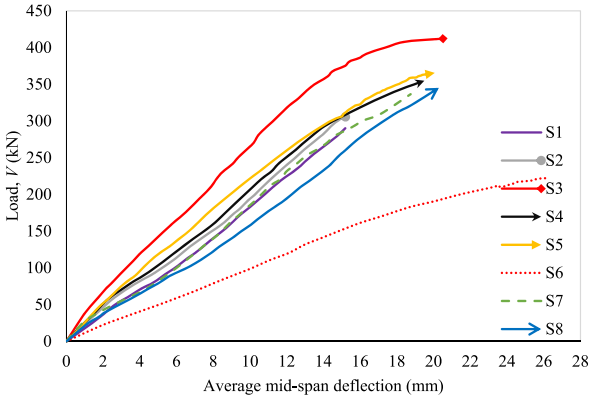

Fig. 11. The comparison of mid-span load-deflection for all specimens.

Table 4
Deflection of the specimens at the mid-span.

Slab	Types of concrete	Average deflection at 100 kN, δ_{100kN} (mm)	Ultimate cracking load, V_{ult} (kN)	Normalized ultimate cracking load, $\frac{V_{ult}}{ud(\rho_1 f_{ck})^{1/3}}$	Average ultimate deflection, δ_{ult} (mm)
S1	NC	6.0	290.1	2.55	15.19
S2	SCC	5.3	305.6	2.60	15.20
S3	SFRSCC	3.2	412.1	3.29	20.51
S4	SFRSCC/SCC	4.5	354.9	2.95	19.50
S5	SFRSCC/SCC	4.1	365.6	3.07	20.07
S6	SFRSCC	10.2	222.3	2.98	26.26
S7	SCC	6.0	336.5	2.77	18.75
S8	SCC	6.3	345.2	2.83	20.29

which the shear reinforcement is arranged in an orthogonal layout, used in this study to avoid a complex configuration, only ensured an increase in strength. However, this configuration did not provide enough coverage to control crack propagation. Cracking is one of the causes of stiffness degradation, and in this case, steel reinforcement is not as effective as fibre reinforcement in controlling crack propagation. As a result, the specimens S7 and S8 reinforced with steel reinforcement were less stiff and deformed more than the specimens reinforced with fibre reinforcement.

The normalized ultimate cracking load, $\frac{V_{ult}}{ud(\rho_1 f_{ck})^{1/3}}$ (where u is the control perimeter in a distance of 2 d from the column face, d is the effective depth, ρ_1 is a flexural reinforcement ratio and f_{ck} is the cylinder compressive strength of concrete) for each specimens is tabulated in Table 4. As expected, the specimens that are cast with SFRSCC show a significant improvement in normalized punching shear. This includes specimen S6, which is thinner than the other specimens. It is evident that the steel fibre reinforcement was suitable to be used regardless of the slab thickness. On the other hand, the performance of specimens reinforced with stirrup and WIB was slightly lower than that of the ones cast with SFRSCC. As these specimens tested in this study were thinner than the suggested depth by EC2 [27], it could not be denied that the performance of steel shear reinforcement such as stirrups and WIB was affected due to the

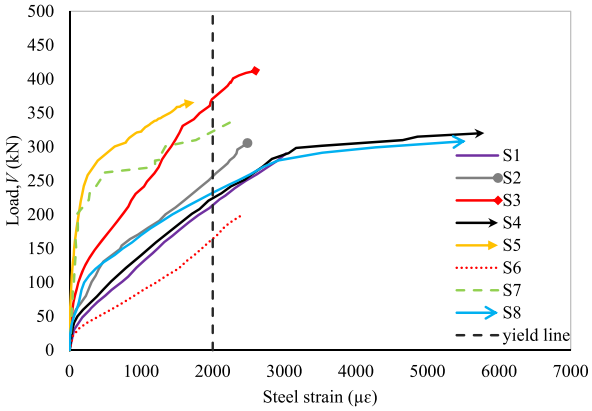

Fig. 12. The load-strain relationship in bottom reinforcement near to column face.

anchorage quality. This is also consistent with ACI-318 [5], which states that the steel shear reinforcement must be properly anchored in order for it to be fully effective. This can be explained by using the "strut and tie" model to analyse the slab. The limited thickness of the RC slab caused the stiffness of this region to be too weak to develop strut-and-tie forces, which disturbed the transmission of the variation of stresses from the longitudinal reinforcement to the vertical branches of the stirrups [19].

3.2. Performance of reinforcement in reinforced concrete flat slabs

Initially, the bottom bars were provided in the reinforced concrete flat slab to avoid flexural failure. This approach is supported by previous research, which has shown that providing steel fibre only in the slab was insufficient to avoid the flexural failure [31,32]. Figs. 12 and 13 illustrate the measured strains of the bottom reinforcement against the applied load, with locations at 0.5d and 2d from the column face, to evaluate the performance of the flexural reinforcement. As can be seen in Fig. 12, the strain in the flexural reinforcement in all specimens reached the yield value prior to failure. This shows that the plastic hinge region is formed near to the column face, which enables the redistribution of moments within the slab and leads to yield lines radiating from the centre. This is also in agreement with the findings reported by Kotsovos and Pavlovic [33] and Farhey et al. [34], who observed the flexural cracking and bar yielding before punching shear failure occurred.

The strains in flexural reinforcement at an early stage were relatively small, as the tension zone of concrete bears the load. As the applied load increased, the strains on the flexural reinforcement also significantly increased due to the formation of the crack on the tension face of the slab. The strains increased in a non-linear relationship as the applied load increased. The graph slowly flattened due to the formation of a punching cone. The measured strain of flexural bar in fibre reinforced concrete specimens shows lower value than the flexural bar in plain concrete specimens. For instance, at the strain reading of 2000 $\mu\varepsilon$, S2 (plain concrete specimen) shows reading of 255 kN, while that in S3 (fibrous specimen) is 370 kN. This shows that the steel fibre in the SFRSCC actively worked to resist the shear load, therefore, the flexural bar absorbed less bending stress. Furthermore, the steel fibre in the concrete matrix delayed the yielding of the flexural bar by providing more strength and post-cracking through its bridging effect. It is worth noting that the strain gauge reading of specimen S4 in Fig. 12 was cut off at 320 kN because the strain gauge near the column face suddenly malfunctioned before the specimen failed. Regardless, the discussion is unaffected because the bar has been yielded.

The measured reading of the strain gauge installed in the third row of the shear reinforcement is shown in Fig. 14. As can be seen from the strain gauge's measured strain reading at the beginning of the crack, it is reasonable to assume that the shear reinforcements are not yet fully functional. The increment of the punching shear capacity and the ductility of the specimens show that both shear reinforcements were fully utilised during the development of the shear cracks, by transferring the shear force across the shear crack and delaying the widening of the shear crack. As the applied load increased, inclined cracks continued to propagate away from the column through the WIB and stirrup in the other rows. The measured strain in the stirrup is higher than the strain reading in WIB due to the position of the strain gauge. In further explanation, the location of the ultimate punching cone of slab S8 occurred at a distance of 132 mm from the column face, which did not intersect the third row of the WIB. Meanwhile, the ultimate punching cone of slab S7 occurred 372 mm from the column face, therefore, the cracks intersected the third row of the stirrup. However, it is believed that WIB can work more effectively by decreasing the spacing in radial and tangential directions as the ultimate load of S8 is higher than S7.

3.3. Comparison of strain on concrete surface

The typical strain development of the specimen's surface is illustrated in Figs. 15 and 16. A total of four strain gauges were used to measure the strains on the bottom surface (tension face) of the slabs, which were located at 2d and 3d in both principal directions. The strain readings on the tension face of the slabs were an indicator of crack formation in the slab. The measured strain had exceeded 3500με when the concrete crushed. However, the measured strains depended on the location of the strain gauge as well as the formation of cracks. Therefore, these reported strain readings should not be taken as a strict representation of the behaviour of the slab.

The strain readings shown by each slab prior to the first crack are quite similar, indicating that the presence of steel fibres in the concrete matrix has an insignificant effect on the slab's first cracking capacity. The strain reading increased proportionally to the applied load. The curves of the strain start to deviate after the event of the first crack. As can be seen from the measured strains in Fig. 15, fibrous slabs (S3, S4, S5, and S6) had lower strain readings than non-fibrous slabs (S1, S2 and S7). The effect of steel fibre inclusion may explain this disparity. Due to the presence of steel fibre in the concrete matrix, all fibrous slabs failed in a ductile manner, with a gradual failure mechanism governed by the main reinforcement's elongation.

Figs. 15 and 16 show that the measured strain in slabs S6 (a thinner fibrous specimen) and S8 (a slab reinforced with WIB shear reinforcement) were both low. This is due to the fact that the circumferential cracks in both slabs occurred at a distance of less than 2d from the column face, which has not yet reached the location of the strain gauge. Only the control specimens, S1 and S2, showed very high measured strain in Fig. 16 because the circumferential cracks in both specimens occurred near 3d from the column face. This is also true of the slab S7, which was reinforced with shear stirrups.

3.4. Comparison of cracking patterns

The failure of the flat slab occurred due to the development of diagonal cracks with various inclinations developed along the depth of the slab, from the column face on the compression side of the slab to the circumferential crack on the tension side of the slab, resulting in the formation of a punching cone. Most of the slabs show the same pattern of cracks on the tension face and no concrete crushing was observed on the compression face of the slab (only load patch indention was formed on the compression side of the slab). After the respective ultimate loads were reached in all specimens, the column stub (load patch) clearly punched through the slab. A grid type of crack occurred under the loading area and tangential cracks spread out from the loading area toward the corners of the slab due to the bending moment.

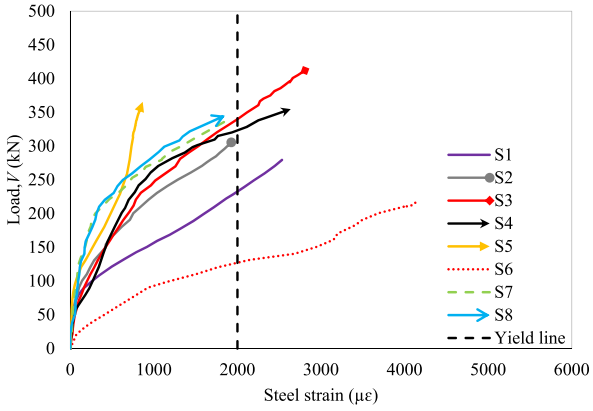

Fig. 13. The load-strain relationship of the bottom reinforcement at 2.0 d from the column face.

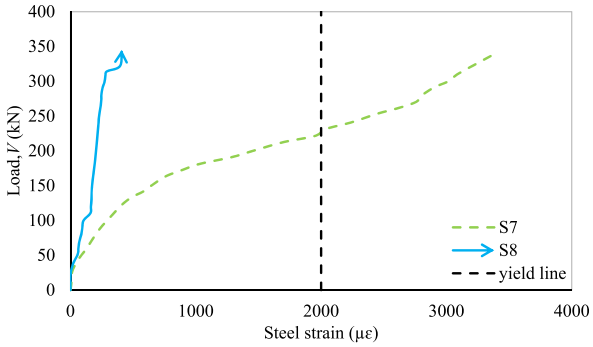

Fig. 14. The load-strain relationship between the stirrup in specimen S7 and the welded inclined bar in specimen S8.

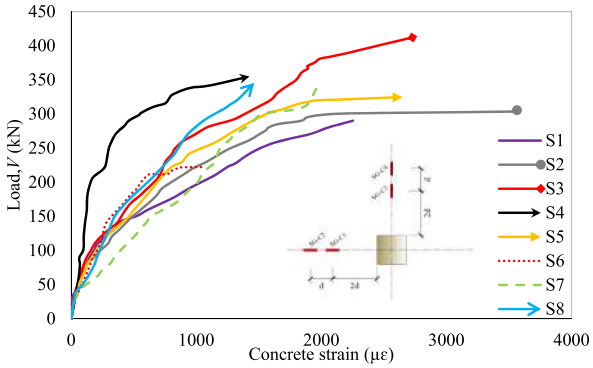

Fig. 15. The load-concrete strain relationship at 2.0d from the column face.

The crack pattern on the tension face of the slab could be categorized into two types. The first category was a sudden and brittle failure, where the most significant sign of this failure was the bottom concrete cover spalling off. This type of crack occurred in the slabs without fibre (excluding slab S4); S1, S2, S7 and S8 as shown in Fig. 17. Despite the fact that S4 was a combination of fibre and plain concrete, the circumferential crack occurred in the non-fibrous region, resulting in brittle failure, as shown in Fig. 18 (a). This can be explained by the fact that plain concrete has brittle characteristics. Meanwhile, the inclusion of shear reinforcement in S7 and S8 did not have any significant contribution to the propagation of the cracks. This is because the simplified "beam layout" adopted in this study is only promising in the strength increment and less complex configuration, as well as reducing the labour work. However, this configuration did not provide sufficient coverage to control the propagation of the cracks.

The second type of failure was a ductile failure, which occurred in slabs with fibre reinforcement; S3, S5, and S6, as shown in Fig. 18 (b). The width of cracks was smaller and their distribution was more uniform as compared to the first category. This is because the steel fibre improves the integrity of the slab in the vicinity of the slab-column connection. Besides, the higher number of fine cracks that

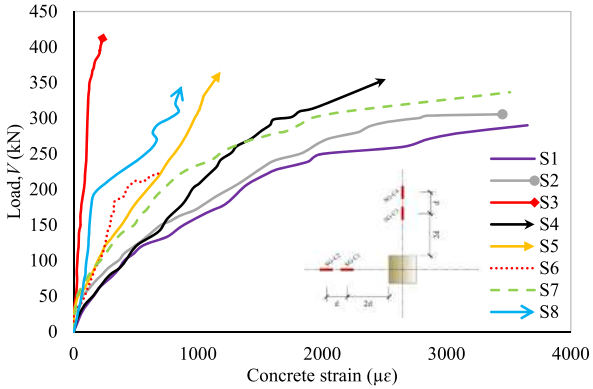

Fig. 16. The load-concrete relationship at 3.0d from the column face.

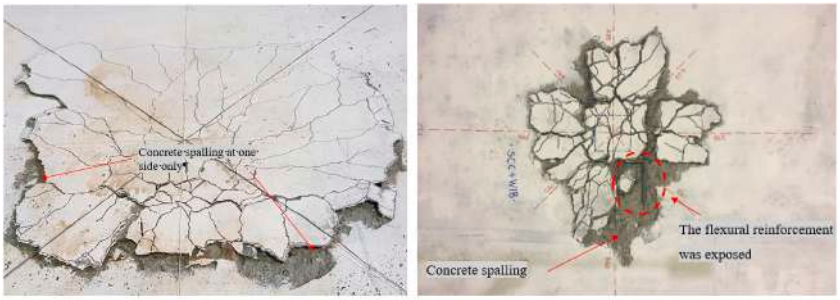

Fig. 17. Brittle failure in slabs that were cast with plain concrete: (a) S2 without shear reinforcement and (b) S8 reinforced with WIB.

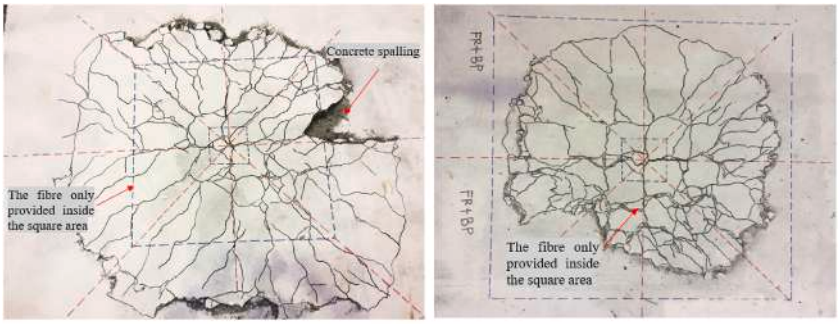

Fig. 18. Comparison of (a) brittle failure in fibrous slab S4 and (b) ductile failure in fibrous slab S5.

existed in the fibrous specimens also presented the ductility behaviour of the slabs. Further, there is no evidence of concrete spalling observed in these three fibrous slabs due to the ability of the steel fibre to bridge the cracks as well as prevent the matrix from spalling. In fibrous specimens, the steel fibre resisted the load until it was completely pulled out of the concrete matrix or broken.

Table 5
The fibre distribution and orientation of core specimen from SFRSCC flat slabs.

Slab	Fibre distribution (%)	Fibre orientation
S3	0.81	0.86
S4	0.67	N/A
S5	0.76	0.82
S6	0.74	0.79

3.5. The effectiveness of fibre reinforcement

The effectiveness of fibre reinforcement in the reinforced concrete flat slab was evaluated based on the distribution and orientation of fibre. This data was used to determine the actual fibre volume fraction in the specimen and the fibre efficiency during post-cracking, which represents the ultimate bridging action. The fibre distribution was calculated based on the total number of fibres that existed in the concrete core extracted from fibrous specimens using Equation (2). The results of fibre distribution are shown in Table 5. In most of the specimens, the measured fibre volume fraction is within 10% of the intended values. Slab S3 shows an average result of 0.81%, which is a little higher than the actual value of 0.75%. This was supported by the experimental result of the slab, which shows the highest strength performance as compared to the others. The uniform distribution of the fibres throughout the specimen was helped by the less congested reinforcement condition in reinforced concrete flat slabs and the self-compacting characteristic of SCC.

Apart from the fibre dosage, the number of effective fibres also depends on its orientation. Steel fibre in a perpendicular orientation to the load will be effective in resisting tension, whereas in an aligned orientation it would not offer any strength contribution. This conclusion creates an interest in knowing the number of effective fibres that cross a cracked section. Therefore, the fibre orientation of the concrete core specimens was calculated using Equation (1) and is tabulated in Table 5. The result shows that the orientation factor for slabs is similar to the orientation factor of two dimensions in the direction of stress. Slab S4 is excluded because the circumferential crack occurred in the non-fibrous region. This finding can be supported by the fact that the orientation of fibres depends on factors like the mixture composition and the rheological characteristics that determine the mobility of fibres in a matrix. Paine [35] demonstrated that using a mechanical vibrator to compact the SFRC mix resulted in randomness in fibre orientation, whereas interaction of fibres in high-flowable concrete such as SCC could be minimised [36]. Thus, in this study, the use of self-compacting concrete as a medium to transport the fibre eliminates the use of the mechanical vibrator, and the lower coarse aggregate content (aggregates hinder the rotation of fibres) in the SCC composition has reduced the negative influence on the orientation of the fibre.

4. Yield line analysis

A yield line analysis is used to estimate the flexural capacity of the reinforced concrete flat slabs and it is based on the yield line pattern described by Elstner and Hognestad [37]. In the moment strength prediction, only the measured yield strength of the flexural reinforcing bars and the cylinder compressive strength of the concrete were considered, while any contribution from the tensile resistance of fibrous concrete was neglected. Furthermore, this yield-line analysis represents a lower-bound estimation of the strength of the slab (assuming punching shear does not govern the slab strength). Therefore, the flexural ultimate load capacity P_{flex}, of the slabs was based on the virtual work done by the actions on the yield lines. The solution was considered as follows:

$$P_{flex} = Km \tag{3}$$

$$K = 8\left(\frac{s}{a-C} - 0.172\right) \tag{4}$$

where s is a side dimension of a square slab, a is the length between supports of a square slab and C is the side of a square column as shown in Fig. 19. The moment capacity per unit length, m was calculated based on the ultimate limit state design consideration of structural elements subjected to bending [27]. The factor of safety for both concrete and steel were neglected.

$$m = \rho f_{yk} b d^2 \left[1 - 0.59\left(\rho f_{yk} / f_{ck}\right)\right] \tag{5}$$

where ρ is the flexural reinforcement ratio, f_{yk} is steel yield strength, f_{ck} is the compressive cylinder strength of concrete, b is the width of the slab and d is the effective depth of the slab.

Based on the tabulated values in Table 6, it can be seen that all the slabs failed before reaching their respective flexural ultimate load capacities. It is known that at the slab-column connection, the flexural and punching shear behaviour are associated with each other [38]. The ratio of the ultimate load capacity of the slab to the flexural ultimate load capacity, computed from the yield-line theory, φ_o is often used as the reference to determine the failure mode of the slabs [39,40]. When the value of $\varphi_o \leq 1$, the punching shear failure mode occurs at the respective slab. Whereas, the slab might experience the flexural mode of failure when $\varphi_o \geq 1$. In this study, all the slabs experienced the punching shear mode of failure as all the value of $\varphi_o \leq 1$. The control specimens show the

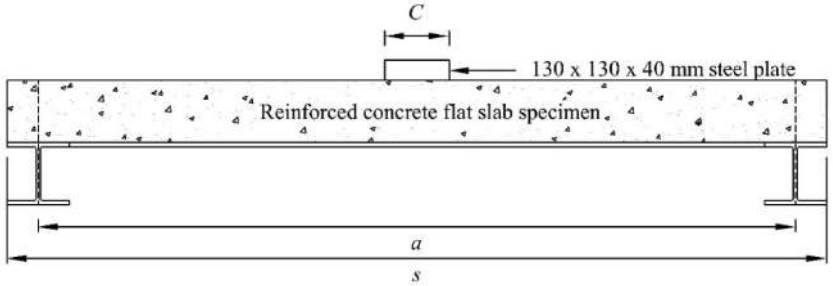

Fig. 19. The dimension of the specimens used to calculate the K value in Equation 4.

Table 6
The flexural ultimate load capacity of RC flat slabs based on a yield-line theory.

Slab	Ultimate load, V_u (kN)	Flexural ultimate load capacity, P_{flex} (kN)	$\varphi_o = \frac{V_u}{P_{flex}}$
S1	290.10	455.90	0.64
S2	305.60	461.32	0.66
S3	412.10	464.24	0.89
S4	354.90	465.03	0.76
S5	365.60	461.70	0.79
S6	222.30	288.16	0.77
S7	336.50	409.76	0.82
S8	345.20	410.41	0.84

lowest value of φ_o, meanwhile the other slabs reinforced with fibre or conventional shear reinforcement show a high value of φ_o. This proved that the additional reinforcement (inclusion of steel fibre or conventional shear reinforcement) in all these slabs has worked effectively in resisting the punching shear load.

5. Conclusion

The following conclusions can be drawn from the results presented.

1. The addition of steel fibre increased the punching shear strength and deformation capacity of the slab. The punching shear resistance of the SFRSCC slabs were 16.1%–34.8% higher than the resistance of the slab with SCC. This is attributable to the fibre bridging action in the concrete matrix and the tension zone of SFRSCC slabs, which participates in carrying the loads and resisting the propagation of cracks.
2. The punching shear resistance of the slab with SFRSCC-0.75 in the central square region bordered at two times the slab effective depth (2d) from the column faces was higher than those of the slab with the SCC and the slabs with stirrup and welded inclined bar (WIB). There were no failures at the interface between the SFRSCC region and the surrounding SCC.
3. The simplified 'beam layout' concept used in the stirrup and WIB arrangements in the slabs was only promising in terms of increasing the strength and simplifying the configuration, but this concept did not provide sufficient coverage for controlling crack propagation as performed by the fibre reinforcement. However, as the slab thickness used in this study was below the suggested thickness in EC2, the performance of the shear reinforcement was also affected by its quality of anchorage. Therefore, further investigation is clearly desirable.
4. The average value of the distribution of the fibre in the RC flat slabs was within 10% of the intended values, while the fibre orientation was greater than the common orientation factor ($\alpha = 0.41$), indicating that the majority of the fibre work effectively in bridging the crack. The less congested reinforcement in reinforced concrete flat slabs and the self-compactability of SCC possibly contributed to the uniform fibre distribution throughout the specimen and less randomness in fibre orientation.
5. The fibre reinforcement has tremendous potential to be employed as a secondary reinforcement in flat slabs based on its capacity to improve shear strength, ductility, and cracking control, as well as ease of configuration.

CRediT authorship contribution statement

Nor Fazlin Zamri: Conceptualization, Methodology, Investigation, Resources, Writing, Visualization. **Roslli Noor Mohamed:** Conceptualization, Methodology, Resources, Writing, Supervision. **Dinie Awalluddin:** Conceptualization, Methodology, Investigation, Resources. **Ramli Abdullah:** Conceptualization, Methodology, Writing, Supervision.

Declaration of competing interest

The authors declare that they have no known competing financial interests or personal relationships that could have appeared to influence the work reported in this paper.

Acknowledgement

The authors gratefully acknowledge the sponsorship provided by Universiti Teknologi Malaysia through the ZAMALAH Scholarship.

References

[1] BS 8110-1, Structural Use of Concrete- Part 1: Code of Practice for Design and Construction, 1997.
[2] N.J. Carino, K.A. Woodward, E.V. Leyendecker, S.G. Fattal, Review of the skyline Plaza collapse, Concr. Int. 5 (1983) 35–42.
[3] N.J. Gardner, J. Huh, L. Chung, Lessons from the Sampoong department store collapse, Cem. Concr. Compos. 24 (2002) 523–529.
[4] S. King, N.J. Delatte, Collapse of 2000 Commonwealth Avenue: punching shear case study, J. Perform. Constr. Facil. 18 (2004) 54–61.
[5] ACI Committee 318, Building Code Requirements for Structural Concrete (ACI 318-08), American Concrete Institute, 2008.
[6] J.L. Anderson, Punching of Concrete Slabs with Shear Reinforcement, Royal Institute of Technology, Bulletin, 1963.
[7] W.G. Corley, N. Hawkins, Shearhead reinforcement for slabs, J. Proc. 65 (1968) 811–824.

[8] A. Elgabry, A. Ghali, Tests on concrete slab-column connections with stud-shear reinforcement subjected to shear-moment transfer, ACI Mater. J. 84 (1987) 433–442.
[9] K. Pilakoutas, X. Li, Alternative shear reinforcement for reinforced concrete flat slabs, J. Struct. Eng. 129 (2003) 1164–1172.
[10] H.G. Park, K.S. Ahn, K.K. Choi, L. Chung, Lattice shear reinforcement for slab-column connections, ACI Struct. J. 104 (2007) 294–303.
[11] L. Nguyen-Minh, M. RovňÁk, T. Tran-Quoc, K. Nguyen-Kim, Punching shear resistance of steel fiber reinforced concrete flat slabs, Procedia Eng. 14 (2011) 1830–1837.
[12] L. Facconi, F. Minelli, G. Plizzari, Steel fiber reinforced self-compacting concrete thin slabs-experimental study and verification against Model Code 2010 provisions, Eng. Struct. 122 (2016) 226–237.
[13] J.A.O. Barros, J.A.B. Antunes, Experimental characterization of the flexural behaviour of steel fibre reinforced concrete according to RILEM TC 162-TDF recommendations, RILEM TC 162 (2003) 77–89.
[14] T.N. Nguyen, T.T. Nguyen, W. Pansuk, Experimental study of the punching shear behavior of high performance steel fiber reinforced concrete slabs considering casting directions, Eng. Struct. 131 (2017) 564–573.
[15] R. Narayanan, I.Y.S. Darwish, Use of steel fibers as shear reinforcement, ACI Struct. J. 84 (1987) 216–227.
[16] N.F. Zamri, R.N. Mohamed, N.H.A. Khalid, S. Mansor, N.A. Shukri, M.S.N. Mahmoor, M.D.K. Awalluddin, Performance of medium strength of steel fibre reinforced self-compacting concrete (SFRSCC), IOP Conf. Ser. Mater. Sci. Eng. 431 (2018) 1–8.
[17] N.F. Zamri, R.N. Mohamed, M.A. Ab Kadir, M.D.K. Awalluddin, S. Mansor, N. Ahmad Shukri, M.S.N. Mahmoor, The flexural strength properties of steel fibre reinforced self-compacting concrete (SFRSCC), Malaysian Constr, Res. J. 6 (2019) 24–35.
[18] Department of Environment (Doe), Concrete Mix Design, UK, 1988.
[19] R.N. Mohamed, Shear Strength of Precast Beam-Half Joints Using Steel Fibre Self-Compacting Concrete, Doct. Phil. Thesis, UK Univ. Nottingham., Nottingham, 2009.
[20] The European Project Group, The European Guidelines for Self-Compacting Concrete Specification, Production and Use, United Kingdom, 2005.
[21] R. Siddique, P. Aggarwal, Y. Aggarwal, Influence of water/powder ratio on strength properties of self-compacting concrete containing coal fly ash and bottom ash, Construct. Build. Mater. 29 (2012) 73–81.
[22] K. Turk, M. Karatas, T. Gonen, Effect of fly ash and silica fume on compressive strength, sorptivity and carbonation of SCC, KSCE J. Civ. Eng. 17 (2013) 202–209.
[23] S. Abdallah, M. Fan, D.W.A. Rees, Effect of elevated temperature on pull-out behaviour of 4DH/5DH hooked end steel fibres, Compos. Struct. 165 (2017) 180–191.
[24] S. Abdallah, M. Fan, D.W.A. Rees, Bonding mechanisms and strength of steel fiber–reinforced cementitious composites: Overview, J. Mater. Civ. Eng. 30 (2018) 1–15.
[25] ASTM C494/C494M, ASTM C494/C494M: Standard Specification for Chemical Admixtures for Concrete, 2013.
[26] BS EN 10002-1, Metallic Materials-Tensile Testing-Part 1: Method of Test at Ambient Temperature, 2001.
[27] BS EN 1992-1-1, Eurocode 2, Design of Concrete Structures — Part 1-1: General Rules and Rules for Buildings, British Standards Institution, 2004.
[28] S.D.B. Alexander, S.H. Simmonds, Punching shear tests of concrete slab-column joints containing fiber reinforcement, ACI Struct. J. 89 (1992) 425–432.
[29] M.H. Harajli, D. Maalouf, H. Khatib, Effect of fibers on the punching shear strength of slab-column connections, Cement Concr. Compos. 17 (1995) 161–170.
[30] D.D. Theodorakopoulos, R.N. Swamy, Ultimate punching shear strength analysis of slab-column connections, Cement Concr. Compos. 24 (2002) 509–521.
[31] J. Michels, D. Waldmann, S. Maas, A. Zürbes, Steel fibers as only reinforcement for flat slab construction - experimental investigation and design, Construct. Build. Mater. 26 (2012) 145–155.
[32] K.H. Tan, A. Venkateshwaran, Punching shear in steel fibre reinforced concrete slabs without traditional reinforcement, IOP Conf. Ser. Mater. Sci. Eng. 246 (2017).
[33] M.D. Kotsovos, M.N. Pavlovic, Ultimate Limit-State Design of Concrete Structures: A New Approach, Thomas Telford, London, 1998.
[34] D.N. Farhey, M.A. Adin, D.Z. Yankelevsky, RC flat slab–column subassemblages under lateral loading, J. Struct. Eng. 119 (1993) 1903–1916.
[35] K.A. Paine, Steel Fibre Reinforced Concrete for Prestressed Hollow Core Slabs, Doctoral Dissertation, University of Nottingham, 1998.
[36] S. Grünewald, F. Laranjeira, J. Walraven, A. Aguado, C. Molins, Improved tensile performance with fiber reinforced self-compacting concrete, RILEM Bookser. 2 (2012) 51–58.
[37] R.C. Elstner, E. Hognestad, Shearing strength of reinforced concrete slabs, J. Proc. (1956) 29–58.
[38] G.I.B. Rankin, A.E. Long, Predicting the punching strength of conventional slab-column specimens, Proc. Inst. Civ. Eng. 82 (1987) 327–346.
[39] M.E. Criswell, N.W. Hawkins, Shear strength of slabs: basic principle and their relation to current methods of analysis, Spec. Publ. 42 (1974) 641–676.
[40] H. Marzouk, A. Hussein, Experimental investigation on the behaviour of high-strength concrete slabs, ACI Struct. J. (1991) 701–713.